

This copy is for your personal, non-commercial use only.

If you wish to distribute this article to others, you can order high-quality copies for your colleagues, clients, or customers by [clicking here](#).

Permission to republish or repurpose articles or portions of articles can be obtained by following the guidelines [here](#).

The following resources related to this article are available online at www.sciencemag.org (this information is current as of July 15, 2010):

Updated information and services, including high-resolution figures, can be found in the online version of this article at:

<http://www.sciencemag.org/cgi/content/full/329/5989/342>

Supporting Online Material can be found at:

<http://www.sciencemag.org/cgi/content/full/329/5989/342/DC1>

This article **cites 30 articles**, 12 of which can be accessed for free:

<http://www.sciencemag.org/cgi/content/full/329/5989/342#otherarticles>

This article appears in the following **subject collections**:

Microbiology

<http://www.sciencemag.org/cgi/collection/microbio>

pattern is largely affected well before metamorphosis. *Pdu-ptc* is also down-regulated (fig. S9), as it is observed in *hh*-mutant flies (16) and vertebrates lacking *shh* expression (17). *Pdu-Gli* (Fig. 2I) stripes are mostly persistent even at high doses of cyclopamine. The specificity of the effects of mid-trochophore cyclopamine treatment on the patterning of the segmental ectoderm is demonstrated by the persistence of gene expression in tissues other than segmental ectoderm. Hence the expression of *Pdu-en* and *Pdu-Lbx* in segmental mesoderm (Fig. 2, F and K, red arrows), the stomodeal expression of *Pdu-hh* and *Pdu-Wnt11* (Fig. 2, E and H, blue asterisks), and the pygidial expression of *Pdu-Wnt11* and *Pdu-Cdx* (Fig. 2, H and L, green asterisks) are maintained, whereas the proctodeal expression of *Pdu-Wnt1* is slightly enlarged (Fig. 2G, green asterisks).

The effect of cyclopamine on *Pdu-hh* stripes must be indirect, if we suppose that the direct targets of Hh signaling are only those cells expressing *Pdu-Gli*, away from segment borders. In *Drosophila* (Fig. 3), *wingless* (*wg*) expression is maintained by Hh signaling in the anterior compartment just anterior to the *en* stripe, whereas *wg* signaling is necessary to maintain *en* and *hh* striped expression in the posterior compartment (18). In *Platynereis*, *Pdu-Wnt1*, the ortholog of *Drosophila wingless* (8), is expressed just anterior to *Pdu-en* and *Pdu-hh* stripes on the other side of segmental grooves. Its strong down-regulation by cyclopamine (Fig. 2G) is consistent with a loop of regulation similar to the one known in *Drosophila*. *Ladybird*, the fly gene orthologous to *Pdu-Lbx*, is expressed in epidermal stripes overlapping *wingless* stripes in the anterior compartment of the epidermis and is positively regulated by *wingless* (19). By contrast, cyclopamine treatment in the annelid does not abolish completely *Pdu-Lbx* stripes in trochophores (Fig. 2K), which suggests that other factors are involved in its maintenance. Another difference between the annelid and the fly is that *Pdu-Wnt1* is not expressed in complete circular stripes in the trochophore (it is during posterior growth) but only in the lateral parapodial field (Fig. 2G). It was thus interesting to look at *Pdu-Smo* regulation of other *Wnt* genes potentially involved in segment formation. *Pdu-Wnt11* is expressed in thick stripes in the posterior halves of segments and is strongly down-regulated by cyclopamine (Fig. 2H). *Pdu-Wnt5* is expressed in the anterior halves of segments and is, in contrast, much more resistant to cyclopamine (Fig. 2J).

Our work demonstrates the involvement of the Hh pathway in segment formation outside of arthropods. It contrasts with earlier studies of *hh* orthologs in annelid species (20, 21). The comparison of the effect of Hh signaling inhibition in *Platynereis* and in insects [i.e., the fruit fly and the coleopteran *Tribolium* (3)] reveals extensive similarities. As in insects, *Platynereis* Hh presumably diffuses anteriorly to maintain *Wnt* signaling anterior to the *hh*-expressing cells (Fig. 3), which may in turn be crucial to maintain segment boundary gene expressions, including *Pdu-hh*.

As in insects, Hh is not necessary in the initial setting of the segmental pattern but is required to maintain this pattern before the morphological appearance of segments. The comparison of segment polarity gene patterns between *Platynereis* and arthropods (Fig. 3) reveals four independent players with remarkably similar expressions: *engrailed*, *Lbx/ladybird*, the Hh pathway, and *Wnt1/wingless* signaling. The most likely explanation of these similarities is that these genes were already playing similar roles in a metamereric protostome ancestor. The alternative explanation would be a parallel recruitment of these genes for similar functions in annelids and arthropods. Because they are not known to be part of a conserved core regulatory network or “kernel” (22) that might have been coopted en bloc, each gene would have been recruited independently, which seems unlikely. Altogether, these four players are expressed in the same spatial relation across the annelid segment boundary as they are across the parasegmental boundary in arthropods (Fig. 3). This suggests that these two boundaries are homologous as was proposed earlier (8). Therefore, the segmented exoskeleton of the arthropods must have evolved out of frame with the ancestral protostome segmentation (fig. S13). This ancestral protostome segmentation is nowadays “recapitulated” as parasegmental patterning in the embryos of extant arthropods.

References and Notes

1. V. Hatini, S. DiNardo, *Trends Genet.* **17**, 574 (2001).
2. B. Sanson, *EMBO Rep.* **2**, 1083 (2001).
3. L. Farzana, S. J. Brown, *Dev. Genes Evol.* **218**, 181 (2008).
4. M. Pechmann, A. P. McGregor, E. E. Schwager, N. M. Feitosa, W. G. Damen, *Proc. Natl. Acad. Sci. U.S.A.* **106**, 1468 (2009).
5. F. Simonnet, J. Deutsch, E. Quéinnec, *Dev. Genes Evol.* **214**, 537 (2004).
6. S. A. Holley, *Dev. Dyn.* **236**, 1422 (2007).

7. Materials and methods are available as supporting material on Science Online.
8. B. Prud'homme *et al.*, *Curr. Biol.* **13**, 1876 (2003).
9. A. Saudemont *et al.*, *Dev. Biol.* **317**, 430 (2008).
10. M. van den Heuvel, P. W. Ingham, *Nature* **382**, 547 (1996).
11. J. Alcedo, M. Ayzenzon, T. Von Ohlen, M. Noll, J. E. Hooper, *Cell* **86**, 221 (1996).
12. W. Chen, S. Burgess, N. Hopkins, *Development* **128**, 2385 (2001).
13. J. K. Chen, J. Taipale, M. K. Cooper, P. A. Beachy, *Genes Dev.* **16**, 2743 (2002).
14. J. K. Chen, J. Taipale, K. E. Young, T. Maiti, P. A. Beachy, *Proc. Natl. Acad. Sci. U.S.A.* **99**, 14071 (2002).
15. P. R. Steinmetz, F. Zelada-González, C. Burgdorf, J. Wittbrodt, D. Arendt, *Proc. Natl. Acad. Sci. U.S.A.* **104**, 2727 (2007).
16. A. Hidalgo, P. Ingham, *Development* **110**, 291 (1990).
17. J. P. Concordet *et al.*, *Development* **122**, 2835 (1996).
18. S. DiNardo, J. Heemskerk, S. Dougan, P. H. O'Farrell, *Curr. Opin. Genet. Dev.* **4**, 529 (1994).
19. K. Jagla *et al.*, *Development* **124**, 91 (1997).
20. D. Kang *et al.*, *Development* **130**, 1645 (2003).
21. E. C. Seaver, L. M. Kaneshige, *Dev. Biol.* **289**, 179 (2006).
22. E. H. Davidson, D. H. Erwin, *Science* **311**, 796 (2006).
23. We acknowledge the following agencies for funding: the CNRS, University Paris-Diderot and the Agence Nationale de la Recherche (France) (ANR grant BLAN-0294); the Max F. Perutz Laboratories (MFPL) funds and the Austrian Science Fund (FWF) START award (AY0041321), the French Research Ministry and the Fondation pour la recherche médicale (FRM) for fellowships (N.D.); the Boehringer Ingelheim Foundation and the Marie Curie Research Training Networks ZOONET (MRTN-CT-2004-005624) for fellowships (K.T.R.). We also thank the platform ImagoSeine staff for help in confocal imagery. GenBank accession numbers for the gene sequences newly identified in this study are HM179271 to HM179276.

Supporting Online Material

www.sciencemag.org/cgi/content/full/329/5989/339/DC1
Materials and Methods
SOM Text
Figs. S1 to S13
References

1 March 2010; accepted 24 May 2010
10.1126/science.1188913

Chemoattraction to Dimethylsulfoniopropionate Throughout the Marine Microbial Food Web

Justin R. Seymour,^{1,2,3*} Rafel Simó,⁴ Tanvir Ahmed,¹ Roman Stocker¹

Phytoplankton-produced dimethylsulfoniopropionate (DMSP) provides underwater and atmospheric foraging cues for several species of marine invertebrates, fish, birds, and mammals. However, its role in the chemical ecology of marine planktonic microbes is largely unknown, and there is evidence for contradictory functions. By using microfluidics and image analysis of swimming behavior, we observed attraction toward microscale pulses of DMSP and related compounds among several motile strains of phytoplankton, heterotrophic bacteria, and bacterivore and herbivore microzooplankton. Because microbial DMSP cycling is the main natural source of cloud-forming sulfur aerosols, our results highlight how adaptations to microscale chemical seascapes shape planktonic food webs, while potentially influencing climate at the global scale.

Marine plankton inhabit heterogeneous microscale seascapes (1) where chemical cues allow motile organisms to exploit nutrient patches (2, 3), locate mutualistic partners or hosts (4), and select or avoid prey (5). Dimethyl-

sulfoniopropionate (DMSP) is a phytoplankton-produced solute, which can constitute up to 10% of total cell carbon (6). It is released into the water column via point source events, including exudation, grazing, and cell lysis (6). These events

generate submillimeter, diffusing DMSP pulses that may act as chemical hot spots for microbes that use DMSP as a source of carbon and sulfur (7, 8). Although DMSP represents a potent direct or indirect [by transformation into dimethylsulfide (DMS)] foraging cue for sea urchins, coral-reef fish, procellariiform birds, penguins, and seals (9–12), its role as a chemical cue among marine microorganisms remains unclear. Some bacterioplankton exhibit attraction to DMSP (4, 13), but it has also been suggested that this compound is involved in a grazing-deterrence mechanism in phytoplankton (14, 15). These largely unresolved and apparently contradictory ecological functions of DMSP are likely to play important roles in global sulfur biogeochemistry. Oceanic cycling of DMSP into volatile DMS and the emission and subsequent oxidation of DMS in the atmosphere shape the atmospheric radiative balance by affecting the formation and albedo of clouds (16). Therefore, a potentially large and direct influence of the marine biosphere on climate is ultimately mediated by microbial interactions at the microscale.

We studied the chemotactic behavioral response of seven species of marine microbes by using a microfluidic system (fig. S1) (17, 18) to create ephemeral, submillimeter diffusing patches of DMSP and related compounds, including DMS, dimethylsulfide (DMSO), and glycine betaine (GBT) (Fig. 1; Fig. 2, A to D; and fig. S2), all of which are ubiquitous in the pelagic ocean. The spatiotemporal scales of the chemical patches produced were congruent with release events in the ocean. DMS and DMSO are DMSP degradation products (6), whereas GBT is analogous to DMSP in chemical structure and physiological function (19). Strong chemotactic responses toward DMSP and GBT were displayed by five organisms, which is consistent with the structural analogy between the compounds and the fact that they share membrane transport systems in heterotrophic bacteria and some phytoplankton (7, 8). Positive, albeit weaker, attraction to DMS and DMSO occurred, in line with the observation that these compounds are less biologically labile than DMSP (6, 7). Positive responses were characterized by dense accumulations of cells within chemical micropatches, often occurring in less than 30 s (Fig. 2 and fig. S2). Although negligible chemotactic responses (Fig. 1 and fig. S2) or repulsion (e.g., Fig. 2D) were observed in some instances,

positive chemotaxis was observed in 74% of tested cases, indicating that DMSP and related chemicals are potent chemoattractants across multiple trophic levels in the marine microbial food web. We measured the relative strength of the response using a chemotaxis index, I_C , that quantifies the magnitude of the accumulation of organisms within the chemical patch, and we estimated the increase in integrated chemical exposure due to chemotaxis with an exposure index, I_E (18) (fig. S3). Strong responses led to >65% enhancement in exposure to these compounds (Fig. 1), which, in the ocean, will confer a substantial advantage to chemotactic foragers.

DMSP is produced by many microalgal species, for which it plays multiple physiological roles (6). On the other hand, for non-DMSP-producing autotrophs, uptake and assimilation of DMSP may represent a source of reduced sulfur (8, 20). We found that motile phytoplankton can use chemotaxis to actively seek out localized DMSP pulses. The chlorophyte *Dunaliella tertiolecta* [The Provasoli-Guillard National Center for Culture of Marine Plankton (CCMP)1320] and the prasinophyte *Micromonas pusilla* (CCMP2709) both exhibited substantial chemoattraction to DMSP, reaching I_C values of 1.94 and 4.96, respectively (Fig. 1; Fig. 2, B and D; and fig. S2, D and E). *D. tertiolecta* was also attracted to DMS (Fig. 1, Fig. 2D, and fig. S2E). In contrast, the motile cyanobacterium *Synechococcus* WH8102 did not exhibit chemotaxis to any tested compound ($I_C < 0$) (Fig. 1 and fig. S2C), despite its ability to take up DMSP (20). The *M. pusilla* strain used here actively assimilates DMSP sulfur into macromolecules (18) and utilizes chemotaxis to increase its exposure to DMSP by up to 41% (Fig. 1).

The strong response of *D. tertiolecta* is intriguing because [^{35}S]DMSP uptake experiments indicate that this strain does not take up or assimilate DMSP (18). Instead, it cleaves DMSP extracellularly to produce DMS (fig. S4). This, along with the strong attraction toward DMS, suggests an ecophysiological requirement for DMS. *Dunaliella* sp. have been shown to photooxidize DMS into DMSO (21), but in DMS-addition experiments with *D. tertiolecta* (CCMP1320), we did not observe any degradation or incorporation of DMS (fig. S5). Hence, in this case, an as-yet-undefined incentive other than sulfur incorporation drives chemotaxis to DMSP. Therefore, chemoattraction to DMSP by phytoplankton can be driven by divergent ecophysiological demands: Some phytoplankton use chemotaxis toward DMSP to assimilate it; others exhibit chemotaxis before extracellular transformation of the compound. Furthermore, because predators are also attracted to DMSP patches (e.g., Figs. 2C and 3) the ecological benefits of these responses must outweigh the potential cost of increased exposure to grazing.

DMSP produced by phytoplankton also supports a significant proportion of the carbon and sulfur requirements of marine heterotrophic bacteria (7, 22). Between 30 and 90% of oceanic DMSP is metabolized by bacteria, which either demethylate DMSP to assimilate part of its sulfur as methanethiol (MeSH) or cleave DMSP to release DMS (7, 8, 23). We quantified the chemotactic response of the α -proteobacterium *Silicibacter* sp. (TM1040) and the γ -proteobacterium *Pseudoalteromonas haloplanktis* [American Type Culture Collection (ATCC) 700530]. Both *Silicibacter* sp. (TM1040) and some strains of *P. haloplanktis* demethylate DMSP (24, 25). *P. haloplanktis*

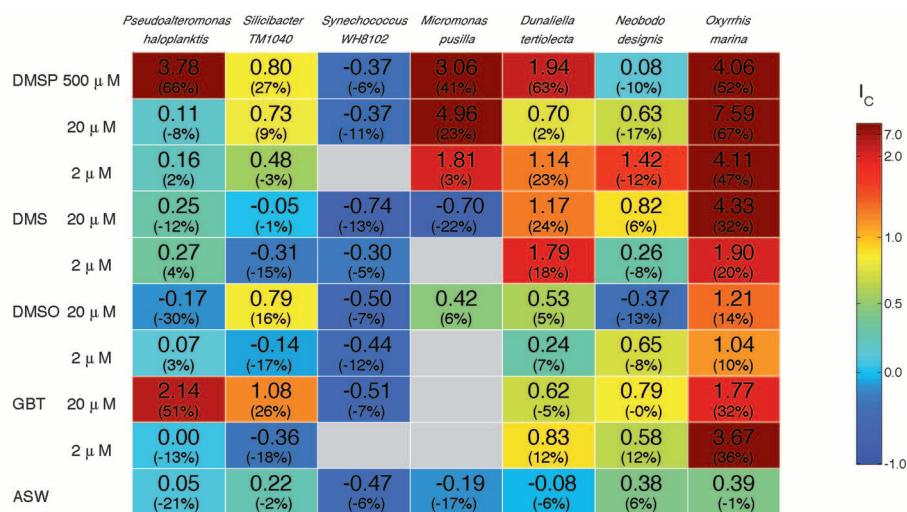


Fig. 1. The strength of the attraction to pulses of DMSP and related compounds, as illustrated by the chemotactic index (I_C), which is based on cell distributions, and the exposure index (I_E), which is based on response speed and substrate diffusion rates (18). Both I_C and I_E are population-averaged quantities. The color code and top number in each cell describe maximum I_C values observed during each experiment. Large positive I_C indicates strong chemotactic attraction, whereas $I_C \leq 0$ corresponds to lack of attraction. Numbers in parentheses correspond to the I_E averaged over time (1 to 6 min). Where I_C is large but I_E is small (e.g., *N. designis*), organisms respond strongly but not rapidly. ASW denotes the artificial-seawater-only control. Gray boxes are cases where no data were acquired.

¹Ralph M. Parsons Laboratory, Department of Civil and Environmental Engineering, Massachusetts Institute of Technology, Cambridge, MA 02139, USA. ²School of Biological Sciences, Flinders University, General Post Office Box 2100, Adelaide, South Australia, 5001, Australia. ³Plant Functional Biology and Climate Change Cluster (C3), University of Technology, Sydney, Post Office Box 123 Broadway, New South Wales 2007, Australia. ⁴Institut de Ciències del Mar (ICM), Consejo Superior de Investigaciones Científicas (CSIC) Passeig Marítim de la Barceloneta 37-49, 08003 Barcelona, Catalonia, Spain.

*To whom correspondence should be addressed. E-mail: Justin.Seymour@uts.edu.au

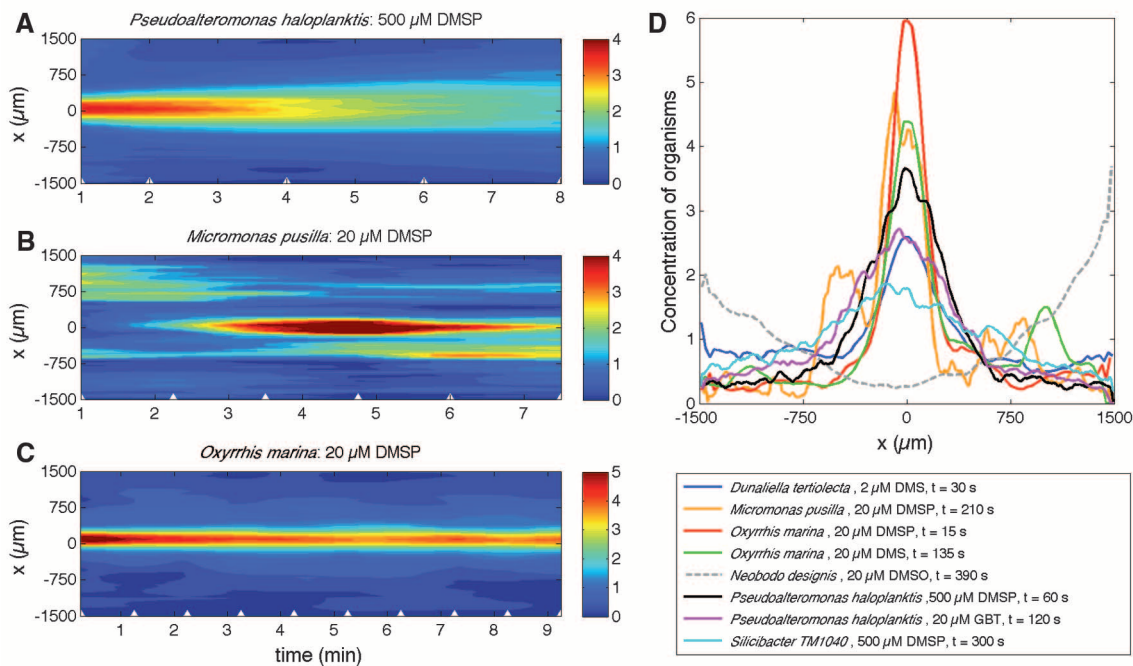
exhibited strong chemotaxis ($I_C = 3.78$) toward high (500 μM) DMSP concentrations (Figs. 1 and 2A), using highly directional swimming to migrate into the DMSP patch with a chemotactic velocity of up to 35 $\mu\text{m s}^{-1}$, or 44% of the mean swimming speed (80 $\mu\text{m s}^{-1}$). Bacterial chemotactic migration rates are typically <10% of swimming speed (26), indicating that DMSP represents

a potent chemoattractant for this strain. In accordance with previous observations (4), TM1040 also exhibited positive, albeit weaker ($I_C = 0.80$), chemotaxis toward DMSP (20 and 500 μM) (Figs. 1 and 2D, and fig. S2B). The rapid response of these bacterial strains resulted in increased exposure to DMSP by up to 66% (Fig. 1). This will impart a significant advantage over nonmotile competitors

in the environment. Such competitive interactions may also determine the balance of DMSP that is demethylated to MeSH or cleaved into DMS, influencing ocean-atmosphere sulfur flux (7, 16).

For microzooplankton, DMSP may be both a resource and an infochemical. DMSP uptake has been shown to supply reduced sulfur to a dinoflagellate grazer via both prey ingestion and

Fig. 2. Chemotactic responses to diffusing patches of DMSP and related compounds. Spatio-temporal distributions of (A) the bacterium *P. haloplanktis*, 500 μM DMSP, (B) the phytoplankter *M. pusilla*, 20 μM DMSP, and (C) the dinoflagellate *Oxyrrhis marina*, 20 μM DMSP. Colors denote cell concentration, normalized to a mean of 1. White triangles indicate times at which cell concentrations across the channel width (x) were measured. (D) Sample concentration profiles of organisms across the microchannel width, normalized to a mean of 1 (measurement times are given in the key). Although attraction was observed for many sulfur



compounds (solid lines), repulsion also occurred (dashed line). For all cases, the pulse was released at time $t = 0$ at the center of the microchannel ($x = 0$) and had an initial width of 300 μm . The full set of spatiotemporal cell distributions is given in fig. S1.

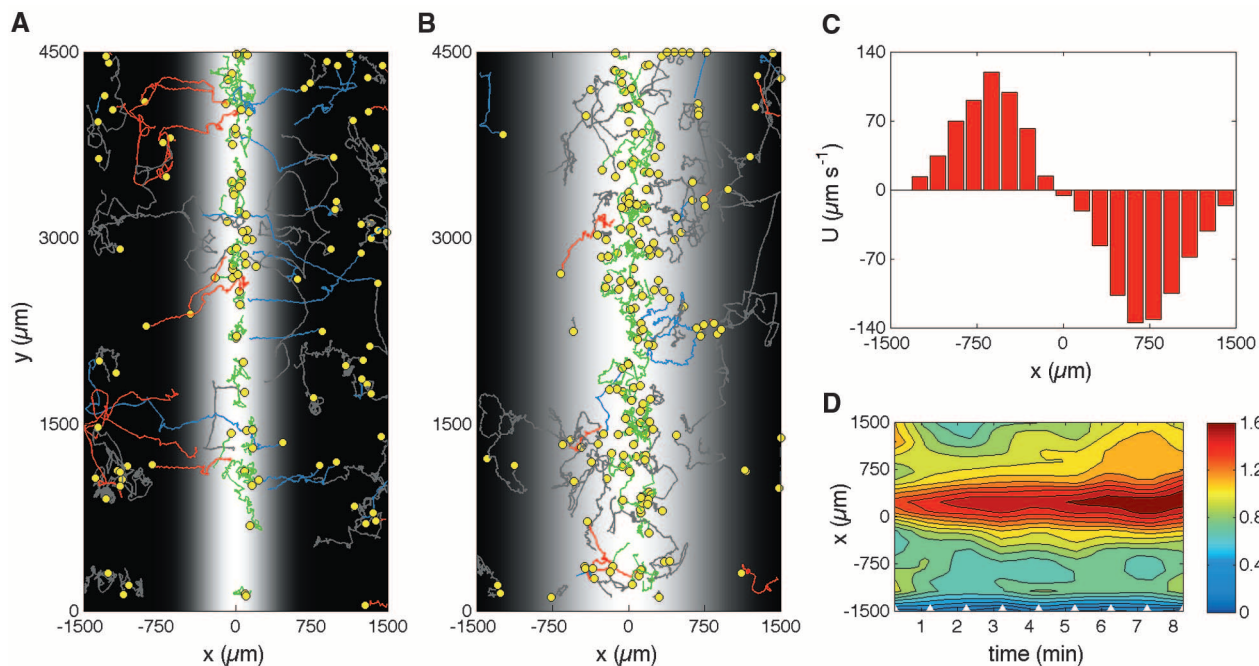


Fig. 3. Swimming behavior of *O. marina* in response to a 20 μM DMSP pulse. (A and B) Trajectories acquired (A) at $t = 15$ s and (B) $t = 255$ s, color-coded as follows: blue, swimming left at $>85 \mu\text{m s}^{-1}$; red, swimming right at $>85 \mu\text{m s}^{-1}$; green, trajectories fully within central 300 μm ; and gray, all others. Yellow dots

indicate starting points, and the gray background is the modeled DMSP concentration field. (C) Chemotactic velocity (i.e., inward speed), U , measured across the channel at $t = 15$ s. (D) Spatio-temporal distribution of the rate of change of direction relative to background value.

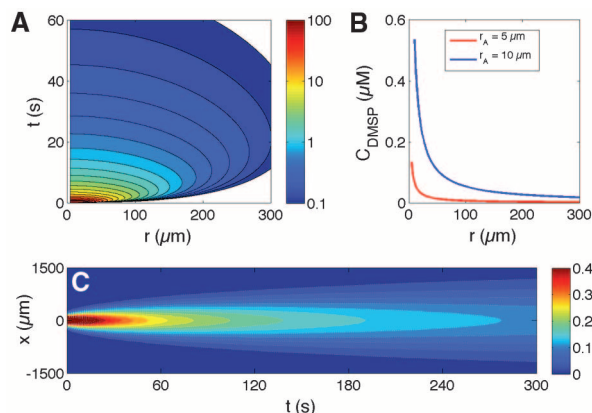
osmotrophic uptake (27). The chemical signature of DMSP produced by phytoplankton could also provide a prey cue for foragers, yet current evidence indicates that DMSP inhibits grazing by microzooplankton (15). To examine this apparent paradox, we measured the foraging response of the herbivorous dinoflagellate *Oxyrrhis marina* (ICM isolate) and the bacterivorous heterotrophic nanoflagellate *Neobodo designis* (CCAP1951/1) to DMSP micropatches. Both species exhibited positive chemotaxis. *N. designis* displayed the highest levels of chemoattraction ($I_C = 1.40$) to low concentrations (2 μM) of DMSP (Fig. 1 and fig. S2F), presumably because of the saturation of chemoreceptors at high DMSP concentrations. *O. marina* exhibited chemotaxis ($I_C = 1.04$ to 7.59) to all tested concentrations of DMSP, DMS, DMSO, and GBT (Fig. 1; Fig. 2, C and D; and fig. S2G), with its response to DMSP the strongest observed among all cases tested ($I_C = 7.59$). *O. marina* showed pronounced shifts in swimming behavior, migrating into DMSP patches with chemotactic velocities of up to $135 \mu\text{m s}^{-1}$, or 35% of the mean swimming speed ($330 \mu\text{m s}^{-1}$) (Fig. 3, A to C), and doubling turning rates once inside the patch to retain position within it (Fig. 3D).

These chemotactic responses by *O. marina* are difficult to reconcile with the hypothesis that DMSP is used by phytoplankton in a chemical defense system against this species (14, 15, 28). This view was derived from observations that bulk additions of 20 μM DMSP reduced grazing rates of *O. marina* on the DMSP-producing phytoplankton *Emiliana huxleyi* (15). In light of the strong attractive responses observed here, we alternatively propose that *O. marina* might utilize DMSP as a prey cue. This is consistent with observations that viral infection of *E. huxleyi*, which will augment DMSP release, increases grazing rates by *O. marina* (29). We suggest that in previous grazing experiments (15), bulk additions of DMSP obscured the microscale chemical signature of individual phytoplankton cells by saturating the system with signal molecules, masking the position of cells, and reducing grazing rates.

Bulk seawater concentrations of DMSP are typically in the nanomolar range (30), whereas phytoplankton internal concentrations can exceed 100 mM (6). Thus, DMSP concentrations will be orders of magnitude higher than background within microzones surrounding individual phytoplankters that leak DMSP because of cell damage or lysis (Fig. 4, A and B). In our experiments, initial concentrations rapidly decreased as patches diffused (Fig. 4C), so that concentrations in the microchannel paralleled those expected around cells in the environment. Phagotrophic grazers responded to pulses with lower DMSP concentrations (2 μM) than were detected by heterotrophic bacteria (20 to 500 μM), potentially allowing grazers to respond from greater distances. A 0.1 μM sensitivity will allow a grazer to detect a stressed, or virus-infected (29), phytoplankton cell exuding DMSP from 50 μm away (Fig. 4B). At the chemotactic velocities observed here, *O. marina* can cover this distance in <0.5 s. In contrast, one-tenth the sensitivity (1 μM) will hardly allow bacteria to detect exuding phytoplankton (Fig. 4B). However, it enables them to detect the lysis of a DMSP-producing phytoplankton cell from $>150 \mu\text{m}$ away and for a total time of >15 s (Fig. 4A), which permits uptake of the DMSP-rich cell lysis products. Therefore, the ecological role of chemotaxis toward DMSP may vary between microorganisms. Foraging microzooplankton could use DMSP chemotaxis as a searching tool to hone in on prey from tens of micrometers away, whereas bacteria might use it to maintain close associations with phytoplankton cells (4) or to exploit cell lysis events (29, 31).

These findings imply that DMSP and related compounds are pervasive chemical cues that drive microbe-microbe interactions within the marine microbial food web and thus extend the importance of these infochemicals from macroorganisms (9–12) to microorganisms. In nature, the chemotactic responses demonstrated here may boost DMSP consumption rates by supporting algal-bacterial mutualism and could enhance DMS production by increasing both microbial exposure to DMSP pulses and grazing rates on

Fig. 4. Chemical micropatch diffusion dynamics. (A) Spatio-temporal variation of the DMSP concentration (μM) following the lysis of a 5- μm radius phytoplankton cell. Distance from the center of the cell is r , time elapsed since lysis is t . (B) Spatial variation of the DMSP concentration with distance from a stressed (18), DMSP-exuding phytoplankton cell, for two cell radii (5 and 10 μm). In (A) and (B), the intracellular DMSP concentration was 100 mM. (C) The initial DMSP concentration in the microfluidic pulses rapidly diffused to considerably lower values. Colors show the computed reduction factor (concentration normalized by the initial concentration in the patch), as a function of time t and distance x across the microchannel.



DMSP-producing prey. These are key regulating processes for ocean-atmosphere DMS flux. This portends that microbial behaviors, played out over microscale chemical landscapes, shape planktonic food webs while potentially influencing climate at global scales.

References and Notes

1. F. Azam, *Science* **280**, 694 (1998).
2. T. Fenchel, *Science* **296**, 1068 (2002).
3. R. Stocker, J. R. Seymour, A. Samadani, D. E. Hunt, M. F. Polz, *Proc. Natl. Acad. Sci. U.S.A.* **105**, 4209 (2008).
4. T. R. Miller, K. Hnilicka, A. Dziedzic, P. Desplats, R. Belas, *Appl. Environ. Microbiol.* **70**, 4692 (2004).
5. A. J. Hartz, B. F. Sherr, E. B. Sherr, *J. Eukaryot. Microbiol.* **55**, 18 (2008).
6. J. Stefels, M. Steinke, S. Turner, G. Malin, S. Belviso, *Biogeochemistry* **88**, 245 (2007).
7. R. P. Kiene, L. J. Linn, J. A. Bruton, *J. Sea Res.* **43**, 209 (2000).
8. M. Vila-Costa *et al.*, *Science* **314**, 652 (2006).
9. K. L. Van Alstyne, G. V. Wolfe, T. L. Freidenburg, A. Neill, C. Hicken, *Mar. Ecol. Prog. Ser.* **213**, 53 (2001).
10. J. L. DeBose, S. C. Lema, G. A. Nevitt, *Science* **319**, 1356 (2008).
11. G. A. Nevitt, *J. Exp. Biol.* **211**, 1706 (2008).
12. G. B. Cunningham, V. Strauss, P. G. Ryan, *J. Exp. Biol.* **211**, 3123 (2008).
13. R. K. Zimmer-Faust, M. P. de Souza, D. C. Yoch, *Limnol. Oceanogr.* **41**, 1330 (1996).
14. G. V. Wolfe, M. Steinke, G. O. Kirst, *Nature* **387**, 894 (1997).
15. S. Strom, G. V. Wolfe, A. Slajer, S. Lambert, J. Clough, *Limnol. Oceanogr.* **48**, 230 (2003).
16. R. Simó, *Trends Ecol. Evol.* **16**, 287 (2001).
17. J. R. Seymour, T. Ahmed, Marcos, R. Stocker, *Limnol. Oceanogr. Methods* **6**, 477 (2008).
18. Materials and methods are available as supporting material on Science Online.
19. D. T. Welsh, *FEMS Microbiol. Rev.* **24**, 263 (2000).
20. R. R. Malmstrom, R. P. Kiene, M. Vila, D. L. Kirchman, *Limnol. Oceanogr.* **50**, 192 (2005).
21. H. Fuse *et al.*, *Biosci. Biotechnol. Biochem.* **59**, 1773 (1995).
22. R. Simó *et al.*, *Aquat. Microb. Ecol.* **57**, 43 (2009).
23. E. C. Howard *et al.*, *Science* **314**, 649 (2006).
24. K. M. Ledyard, E. F. DeLong, J. W. H. Dacey, *Arch. Microbiol.* **160**, 312 (1993).
25. T. R. Miller, R. Belas, *Appl. Environ. Microbiol.* **70**, 3383 (2004).
26. H. C. Berg, D. A. Brown, *Nature* **239**, 500 (1972).
27. V. Saló, R. Simó, M. Vila-Costa, A. Calbet, *Environ. Microbiol.* **11**, 3063 (2009).
28. G. V. Wolfe, *Biol. Bull.* **198**, 225 (2000).
29. C. Evans, W. H. Wilson, *Limnol. Oceanogr.* **53**, 2035 (2008).
30. R. P. Kiene, D. Slezak, *Limnol. Oceanogr. Methods* **4**, 80 (2006).
31. N. Blackburn, T. Fenchel, J. G. Mitchell, *Science* **282**, 2254 (1998).
32. This research was funded by Australian Research Council grant DP0772186 to J.R.S., a Martin Fellowship for Sustainability to T.A., the Spanish Ministry of Science and Innovation project SUMMER to R.Si., funding from La Cambra de Barcelona to R.Si. and R.S., and support from the Hayashi Fund, a Doherty Professorship and NSF grant OCE-0744641-CAREER to R.S. We thank P. Jiménez and A. Calbet for growing and providing *O. marina*, W. M. Durham for preparing *M. pusilla*, Marcos for preparing *N. designis*, and R. Belas for providing *Silicibacter*. We thank S. Strom and J. G. Mitchell for comments on an earlier version of the manuscript.

Supporting Online Material

www.sciencemag.org/cgi/content/full/329/5989/342/DC1
Materials and Methods
Figs. S1 to S7

16 February 2010; accepted 10 June 2010
10.1126/science.1188418